Original Article

Reproducibility of the CT radiomic features of pulmonary nodules: the effects of the CT reconstruction algorithm, radiation dose, and contrast agent

Shou-Xin Yang[1,2], Meng Li[1], Li-Na Zhou[1], Dong-Hui Hou[1], Li Zhang[1], Ning Wu[1,3]

[1]Department of Diagnostic Radiology, National Cancer Center/National Clinical Research Center for Cancer/Cancer Hospital, Chinese Academy of Medical Sciences and Peking Union Medical College, Beijing, China; [2]Key Laboratory of Carcinogenesis and Translational Research (Ministry of Education), Department of Radiology, Peking University Cancer Hospital & Institute, Beijing, China; [3]Department of Nuclear Medicine (PET-CT Center), National Cancer Center/National Clinical Research Center for Cancer/Cancer Hospital, Chinese Academy of Medical Sciences and Peking Union Medical College, Beijing, China

Contributions: (I) Conception and design: SX Yang, L Zhang, N Wu; (II) Administrative support: L Zhang, N Wu; (III) Provision of study materials or patients: SX Yang, M Li, L Zhang; (IV) Collection and assembly of data: SX Yang, M Li, LN Zhou, DH Hou; (V) Data analysis and interpretation: SX Yang, M Li, L Zhang; (VI) Manuscript writing: All authors; (VII) Final approval of manuscript: All authors.

Correspondence to: Li Zhang, MD. Department of Diagnostic Radiology, National Cancer Center/National Clinical Research Center for Cancer/Cancer Hospital, Chinese Academy of Medical Sciences and Peking Union Medical College, No. 17 Panjiayuan Nanli, Chaoyang District, Beijing 100021, China. Email: zhangli_cicams@163.com; Ning Wu, MD. Department of Diagnostic Radiology, National Cancer Center/National Clinical Research Center for Cancer/Cancer Hospital, Chinese Academy of Medical Sciences and Peking Union Medical College, No. 17 Panjiayuan Nanli, Chaoyang District, Beijing 100021, China; Department of Nuclear Medicine (PET-CT Center), National Cancer Center/National Clinical Research Center for Cancer/Cancer Hospital, Chinese Academy of Medical Sciences and Peking Union Medical College, No. 17 Panjiayuan Nanli, Chaoyang District, Beijing 100021, China. Email: cjr.wuning@vip.163.com.

Background: The reproducibility of radiomic features (RFs) is essential in lung nodule diagnosis. This study aimed to prospectively investigate the effects of computed tomography (CT) scanning parameters on the reproducibility of RFs in pulmonary nodules.

Methods: Patients with pulmonary nodules who underwent chest CT scans at the Cancer Hospital of the Chinese Academy of Medical Sciences between July 2018 and March 2019 were prospectively included in the study. Six sequences with three pairs of different scanning parameters, including the reconstruction algorithm [filtered back projection (FBP) *vs.* 50% adaptive statistical iterative reconstruction-V (ASiR-V)], radiation dose (low dose *vs.* standard dose), and contrast agent [contrast-enhanced (CE) CT *vs.* non-contrast enhanced (NE) CT], were used for each patient. When one of the scanning parameters was changed, the other two remained fixed. The nodules were classified into pure ground-glass nodules (pGGNs), part-solid nodules (PSNs), and solid nodules (SNs) according to the nodule consistency. RFs with an intraclass correlation coefficient (ICC) >0.75 were considered to have good retest reliability. All the RF values of the different scanning parameters and nodule consistency were investigated and compared.

Results: A total of 150 pulmonary nodules, including 50 pGGNs, 50 PSNs, and 50 SNs, in 96 patients (mean age: 52±10 years; 62 females) were included in the study. In total, 320 RFs with an ICC >0.75 were evaluated. The proportion of RFs showed significant difference between FBP and 50% ASiR-V, low dose and standard dose, and CE and NE CT scans was 38.4% (123/320), 63.1% (202/320) and 54.1% (173/320), respectively. The radiation dose and contrast agent affected more RFs than the reconstruction algorithm (both P<0.001). In the subgroup analysis of nodule consistency, regardless of changes in the reconstruction algorithms, radiation doses, or contrast agents, the RFs showed significant difference among the pGGNs, PSNs, and SNs (all P<0.001).

Conclusions: The scanning parameters affected the reproducibility of the RFs, and nodules of different

consistency were affected differently. The effects of these parameters should be fully considered in radiomic analysis.

Keywords: Pulmonary nodules; radiomics; reproducibility; computed tomography scanning parameters (CT scanning parameters)

Submitted Sep 22, 2024. Accepted for publication Jan 14, 2025. Published online Feb 24, 2025.
doi: 10.21037/qims-24-2026
View this article at: https://dx.doi.org/10.21037/qims-24-2026

Introduction

Since the concept of radiomics was first introduced in 2012 (1,2), it has captured the interest of scholars from a variety of disciplines. Radiomics is an innovative method for converting imaging examination data into more complex quantitative information using automated algorithms (3-5). Coupled with the advancement of tools for pattern identification, and the expansion of data set sizes, radiomics could improve the predictive accuracy of individualized treatment selection and monitoring in oncology (6,7). Recent studies have shown that radiomics can aid in the differentiation of benign and malignant lung nodules, and in the prediction of lung cancer prognosis (8-15). For example, Lin *et al.* analyzed 180 cases and established a radiomic model for differentiating between benign and malignant sub-centimeter pulmonary nodules (12). Further, in a number of research studies, radiomics has been shown to be effective in predicting gene mutations, such as the epidermal growth factor receptor mutation (16), and Kirsten rat sarcoma viral oncogene homolog mutation (17).

However, despite numerous radiomic studies, radiomics has not yet been established as a clinically useful tool (18). The reproducibility of the results obtained by radiomics is a major research challenge. Several phantom studies have analyzed the effects of computed tomography (CT) acquisition parameters on radiomics using non-uniform CT image acquisition protocols between scanners, and shown that different CT scanners or protocols affect radiomic results (19-22). However, due to the inherent significant differences between phantom material and human tissue, phantom studies cannot truly simulate the radiomic features (RFs) that can be obtained from actual lesions. Few studies have examined the effects of CT reconstruction algorithms, radiation doses, and contrast agents on the RFs of pulmonary nodules using patient images.

Therefore, we conducted a prospective study on individual CT scan acquisition parameters to compare the effects of different reconstruction algorithms, radiation doses, and contrast agents on the reproducibility of RFs in pulmonary nodules. We present this article in accordance with the STROBE reporting checklist (available at https://qims.amegroups.com/article/view/10.21037/qims-24-2026/rc).

Methods

Patient selection

This study was conducted in accordance with the Declaration of Helsinki (as revised in 2013), and was approved by the Medical Ethics Committee of the National Cancer Center/Cancer Hospital, Chinese Academy of Medical Sciences, and Peking Union Medical College (No. NCC19-018/1840). Informed consent was obtained from all patients. Patients who underwent chest CT scans with pulmonary nodules at the Cancer Hospital of the Chinese Academy of Medical Sciences between July 2018 and March 2019 were included in this study (*Figure 1*). To be eligible for inclusion in the study, the patients had to meet the following inclusion criteria: (I) have undergone both non-contrast enhanced (NE) and contrast-enhanced (CE) chest CT examinations; and (II) be known to have or suspected of having pulmonary nodules based on the results of the previous multidetector CT scan. Patients were excluded from the study if they met any of the following exclusion criteria: (I) had CT images that showed no nodules in the lungs; (II) had a lesion size <5 or >30 mm; and/or (III) had a lung nodule boundary that was difficult to segment accurately.

Data reconstruction

All collected CT images were obtained using a 256-Multidetector Computed Tomography (MDCT) (Revolution CT, GE Healthcare, Milwaukee, WI, USA). The scanning range was from the top to the bottom of the lungs. The following scanning parameters were employed:

120 kVp and auto milliampere (pitch: 0.992 and slice thickness: 1.25 mm). The CE scan was performed using a pressure syringe with a peripheral intravenous injection of 85 mL of a non-ionic iodine contrast agent (300 mg/mL) at a rate of 3 mL/s. Scanning began 35 s after the intravenous injection. The three pairs of different scanning parameters were filtered back projection (FBP) and 50% adaptive statistical iterative reconstruction-V (ASiR-V); low dose [noise index (NI) =40] and standard dose (NI =10); and NE CT and CE CT. By altering only one of the three parameters and holding the other two constant, the following three pairs of comparison sequences were obtained: sequence pair 1—the reconstruction algorithm was modified, and the radiation dose and contrast agent remained constant; sequence pair 2—the radiation dose was modified, and the reconstruction algorithm and contrast agent remained constant; sequence pair 3—the contrast agent was modified, and the reconstruction algorithm and radiation dose remained constant. *Figure 2* shows the three pairs of comparison sequences for three different lung nodules.

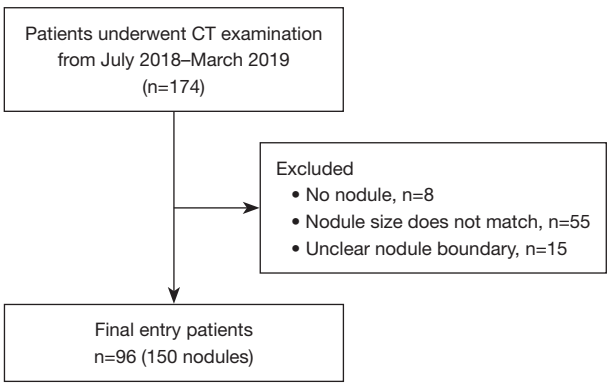

Figure 1 Flow diagram showing patient selection. CT, computed tomography.

Segmentation and RF extraction

All the nodules were segmented manually by a radiologist (S.X.Y.) with five years of diagnostic experience using ITK-SNAP software (http://www.itksnap.org/). The segmentation included the whole nodule, starting from the first layer and continuing to the last layer where the nodules disappeared. In addition, we tried to include the largest edges of the nodules during the segmentation of each layer. In total, 60 pulmonary nodules, including 20 pure ground-glass nodules (pGGNs), 20 part-solid nodules (PSNs), and

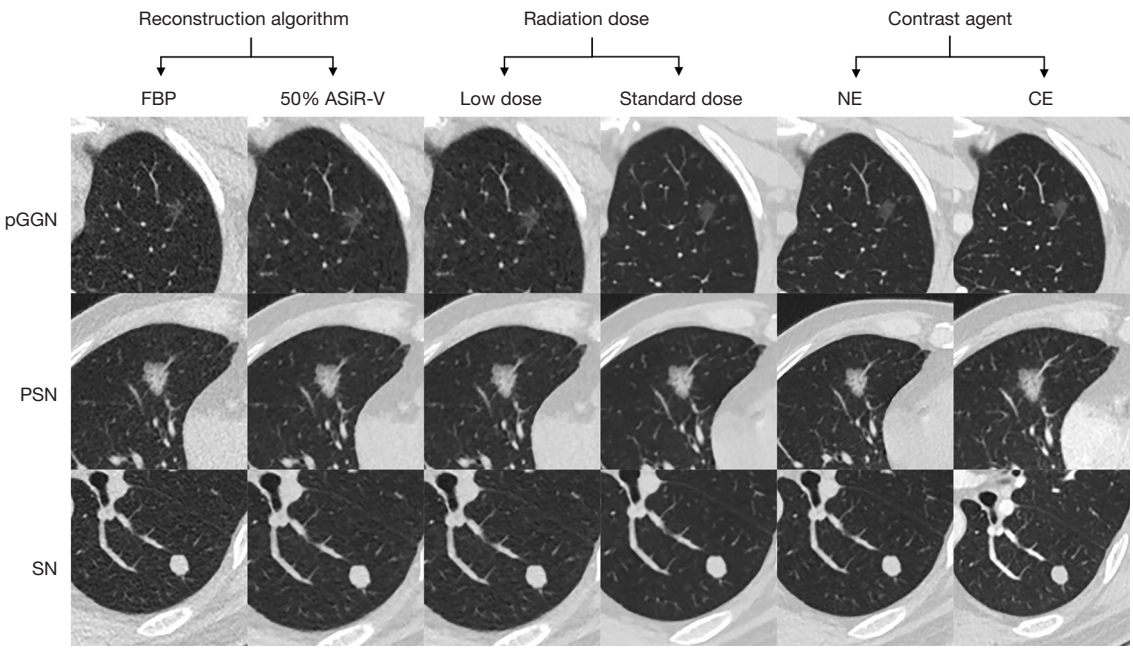

Figure 2 Three pairs of comparison sequences for a pGGN, PSN, and SN. FBP, filtered back projection; ASiR-V, adaptive statistical iterative reconstruction-V; NE, non-contrast enhanced CT; CE, contrast-enhanced CT; pGGN, pure ground-glass nodule; PSN, part-solid nodule; SN, solid nodule; CT, computed tomography.

Table 1 Patient characteristics

Characteristics	pGGNs (n=50)	PSNs (n=50)	SNs (n=50)	All nodules (n=150)
Age, years	48.8±9.3	52.0±10.0	53.4±11.3	52.0±10.0
Sex				
Male	10 (28.6)	12 (28.6)	13 (41.9)	34 (35.4)
Female	25 (71.4)	30 (71.4)	18 (58.1)	62 (64.6)
Nodule size, mm	7.1±3.3	11.5±5.8	7.1±3.3	8.7±4.5
Location				
Right upper lobe	22 (44.0)	15 (30.0)	15 (30.0)	52 (34.7)
Right middle lobe	3 (6.0)	2 (4.0)	7 (14.0)	12 (8.0)
Right lower lobe	8 (16.0)	10 (20.0)	9 (18.0)	27 (18.0)
Left upper lobe	12 (24.0)	12 (24.0)	8 (16.0)	32 (21.3)
Left lower lobe	5 (10.0)	11 (22.0)	11 (22.0)	27 (18.0)

Data are presented as the mean ± standard deviation, or the number (percentage). pGGN, pure ground-glass nodule; PSN, part-solid nodule; SN, solid nodule.

20 solid nodules (SNs), were segmented again by the same radiologist at an interval of 2 weeks to assess consistency. The extraction and analysis of the RFs were performed using the Artificial Intelligence Kit software provided by the GE Healthcare Life Sciences Company (Chicago, IL, USA). Ultimately, 391 RFs were extracted, including 42 histogram, 15 morphological, and 334 texture features (for further details on the 391 RFs, see Figure S1).

Statistical analysis

All the statistical analyses were performed using R software (R foundation for Statistical Computing, Vienna, Austria). The intraclass correlation coefficient (ICC) was used to evaluate the test-retest reliability of the RFs. An ICC of >0.75 indicated good reliability. A paired-sample *t*-test or Wilcoxon test was used to compare the reproducibility of the RFs between different sequences. The Chi-squared test was used to evaluate the difference in the number of RFs that varied with changes in the reconstruction parameters. Benjamini-Hochberg adjustment was applied to control the false discovery rates for multiple comparisons. A P value <0.05 was considered statistically significant.

Results

Patient demographics and RF selection

A total of 150 pulmonary nodules in 96 patients (mean age: 52±10 years; 62 females) were included in the study. The mean nodule size was 8.7±4.5 mm. Of the 150 pulmonary nodules, 52 were in the right upper lobe, 12 were in the right middle lobe, 27 were in the right lower lobe, 32 were in the left upper lobe, and 27 were in the left lower lobe. Among the 150 pulmonary nodules, 50 were pGGNs (mean age: 48.8±9.3 years; 25 females), 50 were PSNs (mean age: 52±10 years; 30 females), and 50 were SNs (mean age: 53.4±11.3 years; 18 females) (*Table 1*).

Of the 391 extracted features, 320 RFs with an ICC >0.75 were ultimately selected for analysis, including 40 histogram, 15 morphological, and 265 texture features. For further details on the 320 RFs, see Table S1.

Effects of reconstruction algorithms, radiation doses, and contrast agents on the RF reproducibility of pulmonary nodules

As *Table 2* shows, when the reconstruction algorithm was modified, there was a significant difference in 38.4% (123/320) of the RFs. When the radiation dose was modified, there was a significant difference in 63.1% (202/320) of the RFs. When the contrast agent was modified, there was a significant difference in 54.1% (173/320) of the RFs. The alteration rates of the RFs due to the radiation dose and contrast agent were essentially the same (P=0.060). The alteration rates of the RFs due to radiation dose and contrast agent were found to be higher

Table 2 Effects of reconstruction algorithms, radiation doses, and contrast agents on the RF reproducibility of pulmonary nodules

Parameters	RFs	Change	Stable	P
Reconstruction algorithm	Total	123 (38.4)	197 (61.6)	<0.001*
	His	14 (35.0)	26 (65.0)	
	Mor	3 (20.0)	12 (80.0)	
	Tex	106 (40.0)	159 (60.0)	
Radiation dose	Total	202 (63.1)	118 (36.9)	0.060**
	His	4 (10.0)	36 (90.0)	
	Mor	4 (26.7)	11 (73.3)	
	Tex	194 (73.2)	71 (26.8)	
Contrast agent	Total	173 (54.1)	147 (45.9)	<0.001***
	His	37 (92.5)	3 (7.5)	
	Mor	5 (33.3)	10 (66.7)	
	Tex	131 (49.4)	134 (50.6)	

Data are presented as the number (percentage). *, reconstruction algorithm *vs.* radiation dose; **, radiation dose *vs.* contrast agent; ***, reconstruction algorithm *vs.* contrast agent. RF, radiomic feature; His, histogram feature; Mor, morphological feature; Tex, texture feature.

than that of the reconstruction algorithm (both P<0.001).

The proportion of histogram features affected by reconstruction algorithm, radiation dose, and contrast agent was 35.0% (14/40), 10.0% (4/40), and 92.5% (37/40) (P<0.001). The proportion of morphological features affected by reconstruction algorithm, radiation dose, and contrast agent was 20.0% (3/15), 26.7% (4/15), and 33.3% (5/15) (P=0.912). The proportion of texture features affected by reconstruction algorithm, radiation dose, and contrast agent was 40.0% (106/265), 73.2% (194/265), and 49.4% (131/265) (P<0.001).

Subgroup analysis on the effects of the reconstruction algorithm, radiation dose, and contrast agent on nodule consistency in RF reproducibility

As *Table 3* and *Figure 3* show, 37.5% (120/320), 12.8% (41/320), and 44.7% (143/320) of the RFs differed significantly between the CT images reconstructed with FBP and those reconstructed with 50% ASiR-V for the pGGNs, PSNs, and SNs, respectively (P<0.001). While 46.3% (148/320), 8.4% (27/320), and 42.2% (135/320) of the RFs differed significantly between the low-dose CT images and standard-dose CT images for the pGGNs, PSNs, and SNs, respectively (P<0.001). Additionally, 50.6% (162/320), 13.8% (44/320), and 41.3% (132/320) of the RFs differed significantly between the CE CT images and NE CT images for the pGGNs, PSNs, and SNs, respectively (P<0.001).

In the GGNs, among the 120 RFs that showed significant differences between the CT images reconstructed with FBP and those reconstructed with 50% ASiR-V, the proportion of histogram, morphological, and texture features were 37.5% (15/40), 6.7% (1/15), and 39.2% (104/265), respectively, and the histogram and texture features showed more variability than the morphological features (P=0.168, 0.033). Among the 148 RFs that showed significant differences between the low-dose CT images and standard-dose CT images, the proportion of histogram, morphological and texture features were 10.0% (4/40), 13.3% (2/15), and 53.6% (142/265), respectively, and the texture features showed the greatest variability (P=0.006, <0.001). Among the 162 RFs that showed significant differences between the CE CT images and NE CT images, the proportion of histogram, morphological, and texture features were 92.5% (37/40), 6.7% (1/15), and 46.8% (124/265), respectively, and the histogram features showed the greatest variability (both P<0.001).

In the PSNs, among the 41 RFs that showed significant differences between the CT images reconstructed with FBP and those reconstructed with 50% ASiR-V, the proportion of histogram, morphological, and texture features were 10.0% (4/40), 6.7% (1/15), and 13.6% (36/265), respectively, and the texture features were found

Table 3 Subgroup analysis of nodule consistency on the effects of the reconstruction algorithm, radiation dose, and contrast agent in the reproducibility of RFs

RFs	Reconstruction algorithm			Radiation dose			Contrast agent		
	Changed	Stable	P	Changed	Stable	P	Changed	Stable	P
pGGNs									
Total	120 (37.5)	200 (62.5)	0.040	148 (46.3)	172 (53.7)	<0.001	162 (50.6)	158 (49.4)	<0.001
His	15 (37.5)	25 (62.5)	0.168$^{\#}$	4 (10.0)	36 (90.0)	>0.999$^{\#}$	37 (92.5)	3 (7.5)	<0.001$^{\#}$
Mor	1 (6.7)	14 (93.3)	0.033$^{\#\#}$	2 (13.3)	13 (86.7)	0.006$^{\#\#}$	1 (6.7)	14 (93.3)	0.006$^{\#\#}$
Tex	104 (39.2)	161 (60.8)	>0.999$^{\#\#\#}$	142 (53.6)	123 (46.4)	<0.001$^{\#\#\#}$	124 (46.8)	141 (53.2)	<0.001$^{\#\#\#}$
PSNs									
Total	41 (12.8)	279 (87.2)	0.628	27 (8.4)	293 (91.6)	0.095	44 (13.8)	276 (86.2)	<0.001
His	4 (10.0)	36 (90.0)	>0.999$^{\#}$	1 (2.5)	39 (97.5)	0.300$^{\#}$	34 (85.0)	6 (15.0)	<0.001$^{\#}$
Mor	1 (6.7)	14 (93.3)	>0.999$^{\#\#}$	3 (20.0)	12 (80.0)	0.933$^{\#\#}$	0 (0.0)	15 (100.0)	>0.999$^{\#\#}$
Tex	36 (13.6)	229 (86.4)	>0.999$^{\#\#\#}$	23 (8.7)	242 (91.3)	0.897$^{\#\#\#}$	10 (3.8)	255 (96.2)	<0.001$^{\#\#\#}$
SNs									
Total	143 (44.7)	177 (55.3)	<0.001	135 (42.2)	185 (57.8)	<0.001	132 (41.3)	188 (58.7)	<0.001
His	8 (20.0)	32 (80.0)	>0.999$^{\#}$	6 (15.0)	34 (85.0)	>0.999$^{\#}$	35 (87.5)	5 (12.5)	<0.001$^{\#}$
Mor	1 (6.7)	14 (93.3)	0.006$^{\#\#}$	1 (6.7)	14 (93.3)	0.006$^{\#\#}$	2 (13.3)	13 (86.7)	0.225$^{\#\#}$
Tex	134 (50.6)	131 (49.4)	<0.001$^{\#\#\#}$	128 (48.3)	137 (51.7)	<0.001$^{\#\#\#}$	95 (35.8)	170 (64.2)	<0.001$^{\#\#\#}$

Data are presented as the number (percentage). $^{\#}$, His *vs.* Mor; $^{\#\#}$, Mor *vs.* Tex; $^{\#\#\#}$, His *vs.* Tex. RF, radiomic feature; His, histogram feature; Mor, morphological feature; Tex, texture feature; pGGN, pure ground-glass nodule; PSN, part-solid nodule; SN, solid nodule.

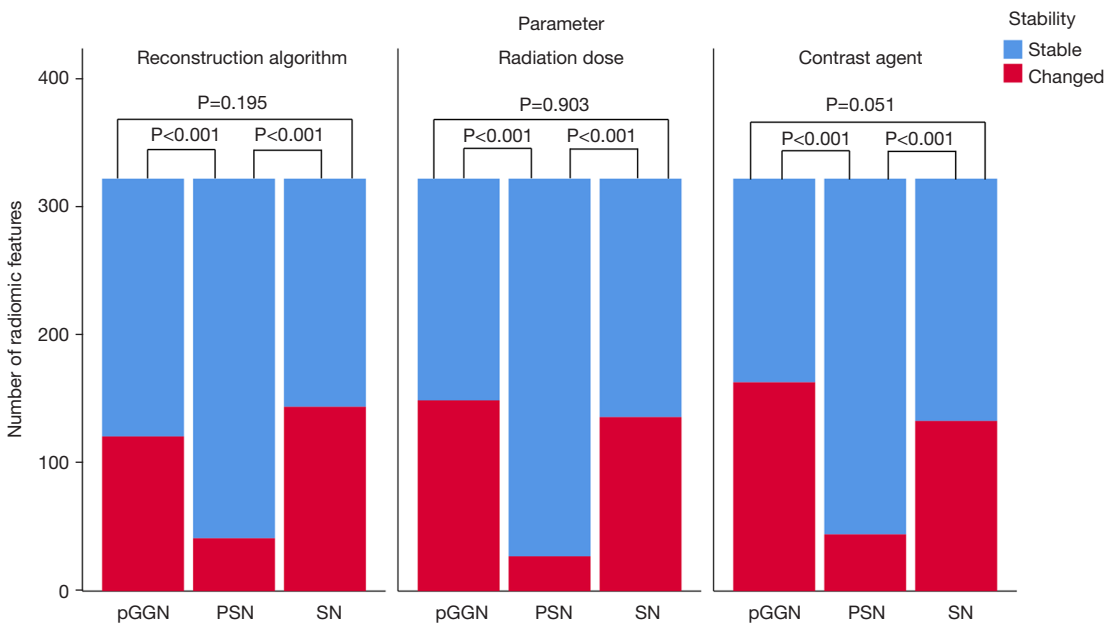

Figure 3 Comparison of the effects of the reconstruction algorithm, radiation dose, and contrast agent on the RFs of pGGNs, PSNs and SNs. pGGN, pure ground-glass nodule; PSN, part-solid nodule; SN, solid nodule; RF, radiomic feature.

to be relatively more affected, but the difference was not statistically significant (P=0.628). Among the 27 RFs that showed significant differences between the low-dose CT images and standard-dose CT images, the proportion of histogram, morphological and, texture features were 2.5% (1/40), 20.0% (3/15), and 8.7% (23/265), respectively and the morphological features were found to be relatively more affected, but the difference was not statistically significant (P=0.095). Among the 44 RFs that showed significant differences between the CE CT images and NE CT images, the proportion of histogram, morphological, and texture features were 85.0% (34/40), 0.0% (0/15), and 3.8% (10/265), respectively, and the histogram features showed the greatest variability (both P<0.001).

In the SNs, among the 143 RFs that showed significant differences between the CT images reconstructed with FBP and those reconstructed with 50% ASiR-V, the proportion of histogram, morphological, and texture features were 20.0% (8/40), 6.7% (1/15), and 50.6% (134/265), respectively, and the texture features showed the greatest variability (P=0.006, <0.001). Among the 135 RFs that showed significant differences between the low-dose CT images and standard-dose CT images, the proportion of histogram, morphological, and texture features were 15.0% (6/40), 6.7% (1/15), and 48.3% (128/265), respectively, and the texture features showed the greatest variability (P=0.006, <0.001). Among the 132 RFs that showed significant differences between CE CT images and NE CT images, the proportion of histogram, morphological and texture features were 87.5% (35/40), 13.3% (2/15), and 35.8% (95/265), respectively, and the histogram features showed the greatest variability (both P<0.001).

Discussion

In this prospective study, 38.4% (123/320), 63.1% (202/320), and 54.1% (173/320) of the RFs showed significant difference between the FBP and 50% ASiR-V, low-dose and standard-dose, and NE CT and CE CT images, respectively. The radiation dose and contrast agent affected more RFs than the reconstruction algorithm (both P<0.001). In the subgroup analysis of nodule consistency, regardless of whichever the reconstruction algorithms, radiation doses, or contrast agents was changed, the proportions of RFs differed significantly among the pGGNs, PSNs, and SNs (all P<0.001).

The findings of our study are aligned with those of previous studies, which reported that the reconstruction algorithm and radiation dose had a significant effect on the RFs (20,23,24). Further, our study showed that the contrast agent also had a significant effect on the RFs of the lung nodules. All the above results provide further evidence that alterations to CT parameters have significant effects on the RFs. Additionally, our findings showed that the radiation dose and contrast agent had a more significant effect on the RFs of the pulmonary nodules than the reconstruction algorithm. Previous studies have also reported differences in the extent to which different parameters affect the RFs of pulmonary nodules. In a study of 89 solid pulmonary nodules >4 mm, Emaminejad *et al.* found that slice thickness had the greatest effect on the RFs, followed by the radiation dose, and reconstruction kernel (24). All these results suggest that more attention needs to be paid to the consistency of scanning parameters in subsequent radiomic studies.

This study also showed that different types of features were affected differently by parameter changes. Compared with the histogram and texture features, the percentage of changes in the morphological features was relatively stable, which is consistent with the findings of previous studies (20,25). A previous study showed that morphological features can provide important clinically relevant information for predicting survival in lung cancer, and head and neck tumors (26). Histogram and texture features play essential roles in diagnosing benign and malignant pulmonary nodules, and predicting tumor sensitivity to immunotherapy (7,9). These results all show that models constructed based on histogram, morphological, and textural features are of great clinical importance. Therefore, stable morphological, histogram, and texture features are crucial in the clinical application of predictive models.

The present study showed that the percentages of RFs differed significantly among the pGGNs, PSNs, and SNs regardless of whichever the reconstruction algorithms, radiation doses, or contrast agents was changed (all P<0.001). For example, the RFs of pGGNs, PSNs, and SNs affected by contrast agents were 50.6% (162/320), 13.8% (44/320), and 41.3% (132/320), respectively. The underlying cause of this outcome may still be predominantly attributed to the notable distinction in the solid components within the pGGNs, PSNs, and SNs. Previous results from both phantom and human studies are consistent with our results (23,27). By analyzing different densities of phantoms, Kim *et al.* found that slice thickness had the greatest effect on the RFs of 100 Hu nodule phantoms, while radiation dose had the greatest

effect on the RFs of –630 Hu nodule phantoms (23). Similarly, Gao *et al.* found a significant difference in the reproducibility of RFs between the SNs and GGNs due to varying doses (27). They suggested that the main reason for the difference was that the radiation dose affected the spatial and density resolution of the images of the GGNs. The results indicated that the effect of varying scanning parameters on RFs of lung nodules was uncontrollable, and that there was a significant difference in the RFs stability on lung nodules of different consistency. For radiomic models constructed by mixing different scanning parameters, it was difficult to identify whether the differences between the benign and malignant nodules were due to tumor heterogeneity, or the effect of different parameters on lung nodules of different consistency. Therefore, future radiomic studies should fully consider the effects of scanning parameters on lung nodules of different consistency, and ensure the stability of the scan parameters to establish highly accurate radiomic models. A previous study showed that applying deep-learning features provided an effective solution, and more diverse and convenient solutions should be explored in the future (28).

Our results showed that the reconstruction algorithm and radiation dose primarily affected the texture features in the pGGNs, PSNs, and SNs, while the contrast agent predominantly affected the histogram features. This discrepancy may be due to the effect of the contrast agent on the RFs within the nodal image. He *et al.* showed that NE scan images contained more diagnostic information than CE images (29). This may be because the contrast agent covers heterogeneity information within the tumor. Given the effect of the contrast agent on feature stability and tumor heterogeneity, further studies need to be conducted to examine how the adverse effects of contrast agents can be avoided in radiomic research.

It should be noted that this study had a number of limitations. First, this study was conducted at a single center with a relatively small sample size, which might have introduced some degree of selection bias. Second, manual segmentation was employed in this study, and the observer variability is likely to exceed that of semi- or fully automatic segmentation. Finally, due to the absence of definitive pathological evidence, we were unable to ascertain which features provide greater diagnostic value in the final analysis. A subsequent prospective study will be conducted to expand the sample size and incorporate pathological results.

Conclusions

Scanning parameters affect the reproducibility of RFs, and nodules of different consistency are affected differently. The effects of these parameters should be fully considered in radiomic analysis.

Acknowledgments

None.

Footnote

Reporting Checklist: The authors have completed the STROBE reporting checklist. Available at https://qims.amegroups.com/article/view/10.21037/qims-24-2026/rc

Funding: This work was supported by the CAMS Innovation Fund for Medical Sciences (Nos. 2022-I2M-C&T-B-076 and 2021-I2M-C&T-B-061), the Beijing Hope Run Special Fund of Cancer Foundation of China (No. LC2022A22), and the National Natural Science Foundation of China (No. 81771830).

Conflicts of Interest: All authors have completed the ICMJE uniform disclosure form (available at https://qims.amegroups.com/article/view/10.21037/qims-24-2026/coif). The authors have no conflicts of interest to declare.

Ethical Statement: The authors are accountable for all aspects of the work in ensuring that questions related to the accuracy or integrity of any part of the work are appropriately investigated and resolved. This study was conducted in accordance with the Declaration of Helsinki (as revised in 2013) and was approved by the Medical Ethics Committee of the National Cancer Center/ Cancer Hospital, Chinese Academy of Medical Sciences, and Peking Union Medical College (No. NCC19-018/1840). Informed consent was obtained from all patients.

References

1. Lambin P, Rios-Velazquez E, Leijenaar R, Carvalho S, van Stiphout RG, Granton P, Zegers CM, Gillies R, Boellard R, Dekker A, Aerts HJ. Radiomics: extracting more information from medical images using advanced feature analysis. Eur J Cancer 2012;48:441-6.
2. Kumar V, Gu Y, Basu S, Berglund A, Eschrich SA, Schabath MB, Forster K, Aerts HJ, Dekker A, Fenstermacher D, Goldgof DB, Hall LO, Lambin P, Balagurunathan Y, Gatenby RA, Gillies RJ. Radiomics: the process and the challenges. Magn Reson Imaging 2012;30:1234-48.
3. Gillies RJ, Kinahan PE, Hricak H. Radiomics: Images Are More than Pictures, They Are Data. Radiology 2016;278:563-77.
4. Cui Y, Yang X, Shi Z, Yang Z, Du X, Zhao Z, Cheng X. Radiomics analysis of multiparametric MRI for prediction of pathological complete response to neoadjuvant chemoradiotherapy in locally advanced rectal cancer. Eur Radiol 2019;29:1211-20.
5. Liu Z, Wang S, Dong D, Wei J, Fang C, Zhou X, Sun K, Li L, Li B, Wang M, Tian J. The Applications of Radiomics in Precision Diagnosis and Treatment of Oncology: Opportunities and Challenges. Theranostics 2019;9:1303-22.
6. Liu Z, Zhang XY, Shi YJ, Wang L, Zhu HT, Tang Z, Wang S, Li XT, Tian J, Sun YS. Radiomics Analysis for Evaluation of Pathological Complete Response to Neoadjuvant Chemoradiotherapy in Locally Advanced Rectal Cancer. Clin Cancer Res 2017;23:7253-62.
7. Sun R, Limkin EJ, Vakalopoulou M, Dercle L, Champiat S, Han SR, Verlingue L, Brandao D, Lancia A, Ammari S, Hollebecque A, Scoazec JY, Marabelle A, Massard C, Soria JC, Robert C, Paragios N, Deutsch E, Ferté C. A radiomics approach to assess tumour-infiltrating CD8 cells and response to anti-PD-1 or anti-PD-L1 immunotherapy: an imaging biomarker, retrospective multicohort study. Lancet Oncol 2018;19:1180-91.
8. Zhou H, Dong D, Chen B, Fang M, Cheng Y, Gan Y, Zhang R, Zhang L, Zang Y, Liu Z, Zheng H, Li W, Tian J. Diagnosis of Distant Metastasis of Lung Cancer: Based on Clinical and Radiomic Features. Transl Oncol 2018;11:31-6.
9. Liu A, Wang Z, Yang Y, Wang J, Dai X, Wang L, Lu Y, Xue F. Preoperative diagnosis of malignant pulmonary nodules in lung cancer screening with a radiomics nomogram. Cancer Commun (Lond) 2020;40:16-24.
10. Hyun SH, Ahn MS, Koh YW, Lee SJ. A Machine-Learning Approach Using PET-Based Radiomics to Predict the Histological Subtypes of Lung Cancer. Clin Nucl Med 2019;44:956-60.
11. Mao L, Chen H, Liang M, Li K, Gao J, Qin P, Ding X, Li X, Liu X. Quantitative radiomic model for predicting malignancy of small solid pulmonary nodules detected by low-dose CT screening. Quant Imaging Med Surg 2019;9:263-72.
12. Lin RY, Zheng YN, Lv FJ, Fu BJ, Li WJ, Liang ZR, Chu ZG. A combined non-enhanced CT radiomics and clinical variable machine learning model for differentiating benign and malignant sub-centimeter pulmonary solid nodules. Med Phys 2023;50:2835-43.
13. Xu H, Zhu N, Yue Y, Guo Y, Wen Q, Gao L, Hou Y, Shang J. Spectral CT-based radiomics signature for distinguishing malignant pulmonary nodules from benign. BMC Cancer 2023;23:91.
14. Digumarthy SR, Padole AM, Rastogi S, Price M, Mooradian MJ, Sequist LV, Kalra MK. Predicting malignant potential of subsolid nodules: can radiomics preempt longitudinal follow up CT? Cancer Imaging 2019;19:36.
15. Mattonen SA, Davidzon GA, Benson J, Leung ANC, Vasanawala M, Horng G, Shrager JB, Napel S, Nair VS. Bone Marrow and Tumor Radiomics at (18)F-FDG PET/CT: Impact on Outcome Prediction in Non-Small Cell Lung Cancer. Radiology 2019;293:451-9.
16. Tu W, Sun G, Fan L, Wang Y, Xia Y, Guan Y, Li Q, Zhang D, Liu S, Li Z. Radiomics signature: A potential and incremental predictor for EGFR mutation status in NSCLC patients, comparison with CT morphology. Lung Cancer 2019;132:28-35.
17. Chen Z, Gao S, Ding C, Luo T, Xu J, Xu S, Li S. CT-based non-invasive identification of the most common gene mutation status in patients with non-small cell lung cancer. Med Phys 2024;51:1872-82.
18. Huang EP, O'Connor JPB, McShane LM, Giger ML, Lambin P, Kinahan PE, Siegel EL, Shankar LK. Criteria for the translation of radiomics into clinically useful tests. Nat Rev Clin Oncol 2023;20:69-82.
19. Mackin D, Fave X, Zhang L, Fried D, Yang J, Taylor B, Rodriguez-Rivera E, Dodge C, Jones AK, Court L. Measuring Computed Tomography Scanner Variability of Radiomics Features. Invest Radiol 2015;50:757-65.
20. Kim H, Park CM, Lee M, Park SJ, Song YS, Lee JH, Hwang EJ, Goo JM. Impact of Reconstruction Algorithms

on CT Radiomic Features of Pulmonary Tumors: Analysis of Intra- and Inter-Reader Variability and Inter-Reconstruction Algorithm Variability. PLoS One 2016;11:e0164924.
21. Shafiq-Ul-Hassan M, Zhang GG, Latifi K, Ullah G, Hunt DC, Balagurunathan Y, Abdalah MA, Schabath MB, Goldgof DG, Mackin D, Court LE, Gillies RJ, Moros EG. Intrinsic dependencies of CT radiomic features on voxel size and number of gray levels. Med Phys 2017;44:1050-62.
22. Zhuo Y, Shen J, Zhan Y, Tian Y, Yu M, Yang S, Ye P, Fan L, Zhang Z, Shan F. Optimization and validation of voxel size-related radiomics variability by combatting batch effect harmonization in pulmonary nodules: a phantom and clinical study. Quant Imaging Med Surg 2023;13:6139-51.
23. Kim YJ, Lee HJ, Kim KG, Lee SH. The Effect of CT Scan Parameters on the Measurement of CT Radiomic Features: A Lung Nodule Phantom Study. Comput Math Methods Med 2019;2019:8790694.
24. Emaminejad N, Wahi-Anwar MW, Kim GHJ, Hsu W, Brown M, McNitt-Gray M. Reproducibility of lung nodule radiomic features: Multivariable and univariable investigations that account for interactions between CT acquisition and reconstruction parameters. Med Phys 2021;48:2906-19.
25. Meyer M, Ronald J, Vernuccio F, Nelson RC, Ramirez-Giraldo JC, Solomon J, Patel BN, Samei E, Marin D. Reproducibility of CT Radiomic Features within the Same Patient: Influence of Radiation Dose and CT Reconstruction Settings. Radiology 2019;293:583-91.
26. Aerts HJ, Velazquez ER, Leijenaar RT, Parmar C, Grossmann P, Carvalho S, Bussink J, Monshouwer R, Haibe-Kains B, Rietveld D, Hoebers F, Rietbergen MM, Leemans CR, Dekker A, Quackenbush J, Gillies RJ, Lambin P. Decoding tumour phenotype by noninvasive imaging using a quantitative radiomics approach. Nat Commun 2014;5:4006.
27. Gao Y, Hua M, Lv J, Ma Y, Liu Y, Ren M, Tian Y, Li X, Zhang H. Reproducibility of radiomic features of pulmonary nodules between low-dose CT and conventional-dose CT. Quant Imaging Med Surg 2022;12:2368-77.
28. Zhan Y, Dai R, Li F, Cheng Z, Zhuo Y, Shan F, Zhou L. Repeatability and reproducibility of deep learning features for lung adenocarcinoma subtypes with nodules less than 10 mm in size: a multicenter thin-slice computed tomography phantom and clinical validation study. Quant Imaging Med Surg 2024;14:5396-407.
29. He L, Huang Y, Ma Z, Liang C, Liang C, Liu Z. Effects of contrast-enhancement, reconstruction slice thickness and convolution kernel on the diagnostic performance of radiomics signature in solitary pulmonary nodule. Sci Rep 2016;6:34921.

Cite this article as: Yang SX, Li M, Zhou LN, Hou DH, Zhang L, Wu N. Reproducibility of the CT radiomic features of pulmonary nodules: the effects of the CT reconstruction algorithm, radiation dose, and contrast agent. Quant Imaging Med Surg 2025;15(3):2309-2318. doi: 10.21037/qims-24-2026